Regioselective Deiodination of Iodothyronamines, Endogenous Thyroid Hormone Derivatives, by Deiodinase Mimics

ARTICLE *in* CHEMISTRY - A EUROPEAN JOURNAL · AUGUST 2014

Impact Factor: 5.73 · DOI: 10.1002/chem.201403248

2 AUTHORS:

Santanu Mondal
Indian Institute of Science
6 PUBLICATIONS **19** CITATIONS
SEE PROFILE

Govindasamy Mugesh
Indian Institute of Science
155 PUBLICATIONS **4,248** CITATIONS
SEE PROFILE

ChemPubSoc Europe

DOI: 10.1002/chem.201403248

CHEMISTRY A European Journal Full Paper

Enzyme Models

Regioselective Deiodination of Iodothyronamines, Endogenous Thyroid Hormone Derivatives, by Deiodinase Mimics

Santanu Mondal and Govindasamy Mugesh*[a]

Abstract: Iodothyronine deiodinases (IDs) are mammalian selenoenzymes that play an important role in the activation and inactivation£ of thyroid hormones. It is known that iodothyronamines (TnAMs), produced by the decarboxylation of thyroid hormones, act as substrates for deiodinases. To understand whether decarboxylation alters the rate and/or regioselectivity of deiodination by using synthetic deiodinase mimics, we studied the deiodination of different iodothyronamines. The triiodo derivative 3,3′,5-triiodothyronamine (T3 AM) is deiodinated at the inner ring by naphthyl-based deiodinase mimics, which is similar to the deiodination of 3,3′,5-triiodothyronine (T3). However, T3 AM undergoes much slower deiodination than T3. Detailed experimental and theoretical investigations suggest that T3 AM forms a weaker halogen bond with selenium donors than T3. Kinetic studies and single-crystal X-ray structures of T3 and T3 AM reveal that intermolecular I···I interactions may play an important role in deiodination. The formation of hydrogen- and halogen-bonding assemblies, which leads to the formation of a dimeric species of T3 in solution, facilitates the interactions between the selenium and iodine atoms. In contrast, T3 AM, which does not have I···I interactions, undergoes much slower deiodination.

Introduction

Iodothyronine deiodinases (IDs) are mammalian selenoenzymes that play an important role in the maintenance of the thyroid-hormone level in the body by employing various activation and deactivation pathways.[1] Type-1 and -2 deiodinases (ID-1 and ID-2) catalyse the conversion of the prohormone L-thyroxine (T4) into biologically active 3,5,3′-triiodothyronine (T3) by means of phenolic ring (5′) deiodination. ID-1 and type-3 deiodinase (ID-3) can convert T4 into the biologically inactive hormone 3,3′,5′-triodothyronine (rT3) by tyrosylring (5) deiodination. ID-1 ID-2, and ID-3 also further catalyse the deiodination of T3 or rT3 to 3,3′-diiodothyronine (3,3′-T2; Scheme 1).[2,3] In addition to deiodination, the thyroid hormones also undergo decarboxylation to produce the corresponding iodothyronamines (TnAMs).

Recent studies have shown that TnAMs act as endogenous signalling molecules, although the exact physiological role of these compounds has not been identified. 3-Iodothyronamine (3-T1 AM) and thyronamine (T0 AM) have been detected in the plasma of various organisms.[4a] When injected into mice, 3-T1 AM induces a decrease in the body temperature (hypothermia) and cardiac output (bradycardia) in pharmacological doses.[4a,b] Interestingly, only the metabolites 3-T1 AM and T0 AM have been detected in plasma, thus indicating that TnAMs, with more iodine atoms, may be deiodinated by IDs. Recently, TnAMs have been identified as substrates of all three types of ID.[5] It should be noted that T4 AM and T3 AM do not undergo 5′-deiodination by ID-1, and the reason for the inability of ID-1 to catalyse phenolic-ring deiodination of these two metabolites is still unknown.

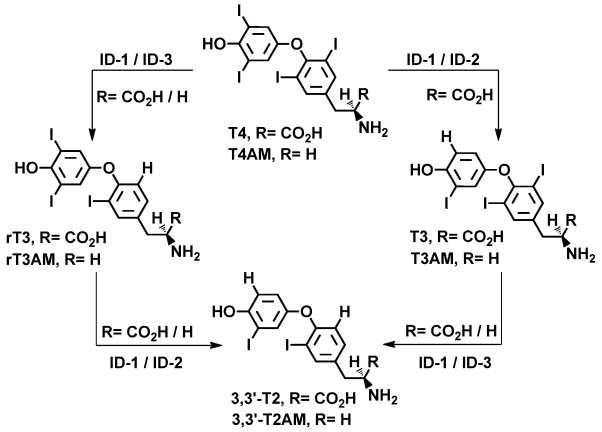

Scheme 1. Deiodination of thyroid hormones (THs) and iodothyronamines (TnAMs) by IDs.

Recently, we showed that naphthyl-based compound **1**, with a thiol and selenol pair, selectively removes iodine atoms from the tyrosyl ring of T4 and T3 to produce rT3 and 3,3′-T2, respectively, under physiologically relevant conditions.[6] Replacement of the selenol group in **1** by a thiol group (i.e., **2**) results in a decrease in the deiodination activity. On the other hand,

[a] S. Mondal, Prof. Dr. G. Mugesh
Department of Inorganic and Physical Chemistry
Indian Institute of Science, Bangalore 560012 (India)
E-mail: mugesh@ipc.iisc.ernet.in

Supporting information for this article is available on the WWW under http://dx.doi.org/10.1002/chem.201403248.

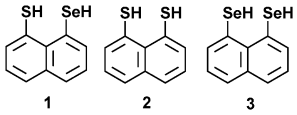

Figure 1. Chemical structures of functional mimics of ID-3.

replacement of the thiol moiety by a selenol group (i.e., **3**; Figure 1) leads to an increase in the deiodination activity, without any change in regioselectivity.[7] As mentioned earlier, the carboxyl group in the β-alanine side chain of T4 affects the deiodination of T4 AM by ID-1 significantly. Deiodination of iodothyronamines was carried out by ID-3 mimics to understand the effect of the carboxyl group on deiodination. Interestingly, the presence of a carboxyl group facilitates the deiodination of T3 by forming a dimer through hydrogen bonding and weak I···I halogen bonding.

Results and Discussion

T4 AM, T3 AM, rT3 AM, and 3,3′-T2 AM were synthesised by following the procedure of Scanlan and co-workers with minor modifications.[8] The deiodination of thyroid hormones and iodothyronamines by means of deiodinase mimics in the presence of dithiothreitol (DTT) was monitored by HPLC. The amount of deiodinated compounds produced in these reactions was quantified by comparing the peak area with that of standard samples. Due to the low solubility of iodothyronamines in phosphate buffer (100 mM, pH 7.00), 20% (v/v) acetonitrile was added to the phosphate buffer. Under these assay conditions, T4 readily underwent selective deiodination of the tyrosyl ring in **5** by **3** to produce rT3. However, when T4 AM was used as a substrate for deiodination, no deiodinated product could be detected probably due to the low solubility of T4 AM in the assay mixture (Figure 2 a). As reported earlier, the deiodination of T3 by **3** produced 3,3′-T2 as the only deiodinated product.[7] Under similar experimental conditions, T3 AM was deiodinated selectively at the tyrosyl ring by **3** to produce 3,3′-T2 AM (Figure 2 b), thus indicating that the removal of the carboxyl group from the β-alanine side chain of T3 does not alter the regioselectivity of the deiodination. On the other hand, rT3 AM and 3,3′-T2 AM did not undergo deiodination, which is in agreement with our earlier reports that rT3 and 3,3′-T2 do not undergo deiodination by **3** under identical experimental conditions.

The deiodination of T4 by a naphthyl-based diselenol has been explained on the basis of co-operative action of halogen bonding (between one of the selenol groups and iodine atom) and chalcogen bonding (between two selenol groups).[9] As T3 AM has three surface-exposed iodine atoms, the selenol group can form halogen bonding with any of the iodine atoms. However, **3** selectively removes one iodine atom from the inner ring of T3 AM to produce 3,3′-T2 AM. Due to anisotropic-charge distribution, halogen atoms contain a significant amount of positive potential (σ-hole) surrounded by a belt of negative potential.[10] The σ-hole in an iodine atom is responsible for the formation of a halogen bond with electron donors. To understand the regioselectivity of deiodination, we carried out DFT calculations. Geometries were optimised by using the B3LYP level of theory and 6-31 + G* basis sets for all the atoms, except iodine for which the 6-311G** basis set was used.

Interestingly, natural-bond orbital (NBO) analysis shows that the natural charges on the two inner-ring iodine atoms of T3 AM are different (0.199 and 0.203 a.u.), and these charges are significantly different from that of the outer-ring iodine atom (0.190 a.u.). Therefore, the σ-hole in the inner-ring iodine atoms can be considered to be more electropositive than the outer-ring iodine atom. To understand the ability of these iodine atoms to form halogen bonds, we used the methyl selenolate ($MeSe^-$) ion as an electron donor. As expected, the $MeSe^-$ ions form halogen bonds with both inner- and outer-ring iodine atoms, which is similar to the formation of halogen bonds between halogen atoms and various other electron donors, as reported earlier.[10,11] Although the C-I-Se bond angle is approximately 180°, the C-Se-I bond angle is approximately 90° (Figure 3). A comparison of the Se···I distances obtained for the outer- and inner-ring iodine atoms indicates that the inner-ring iodine atoms form much stronger halogen bonds with the $MeSe^-$ ion than the outer-ring iodine atom, although both distances are shorter than the sum of the van der Waals radii of the iodine and selenium atoms (3.88 Å). As

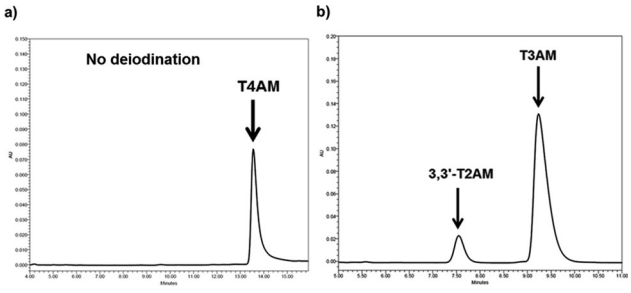

Figure 2. HPLC chromatogram for the deiodination of a) T4 AM and b) T3 AM by **3**. Assay conditions: T4 AM or T3 AM (0.3 mM), **3** (1.2 mM), DTT (15 mM), $NaBH_4$ (30 mM), phosphate buffer (100 mM, pH 7.00), 20% (v/v) acetonitrile, 37 °C.

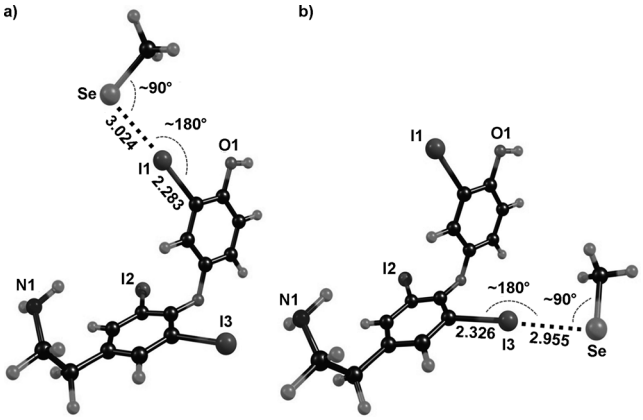

Figure 3. A comparison of the Se···I distances, C–I bond lengths [Å], and C-I-Se and C-Se-I angles [°] for the a) outer-ring and b) inner-ring iodine atoms in the halogen-bonded adducts of T3 AM with the $MeSe^-$ ion.

a result, the inner-ring C–I bond is significantly more elongated (2.326 Å) than the outer-ring C–I bond (2.283 Å). In free T3 AM, the inner- and outer-ring C–I bond lengths were 2.129 and 2.126 Å, respectively.

The halogen-bonding energy between the $MeSe^-$ ion and the inner-ring iodine atom calculated in the gas phase is 59.03 kcal mol^{-1}, which is higher than that observed for the interaction of the $MeSe^-$ ion with the outer-ring iodine atom (46.53 kcal mol^{-1}). The ability of the inner-ring iodine atoms to form stronger halogen bonds with the selenium atom may account for the selective inner-ring deiodination of T3 AM by **3**. Because the removal of an iodine atom from T3 AM decreases the positive potential on the iodine atom, 3,3′-T2 AM does not undergo any further deiodination by **3** (see Table S02 in the Supporting Information). In agreement with this outcome, the interaction energy between the $MeSe^-$ ion and the iodine atoms of 3,3′-T2 AM (51.38 and 51.7 kcal mol^{-1} for the inner and outer rings, respectively) are lower than that observed for the inner-ring iodine atom of T3 AM (59.03 kcal mol^{-1}).

When T4 AM was used as a substrate, no deiodination by **3** was observed. It is known that T4 AM undergoes inner-ring deiodination by ID-1 and ID-3 to produce rT3 AM. However, ID-1 does not catalyse the outer-ring deiodination of T4 AM, although this enzyme can remove an iodine atom from the outer ring of T4 to produce T3. To understand the unexpected behaviour of T4 AM towards **3**, we carried out DFT calculations on T4 AM and the $MeSe^-$ ion. Interestingly, an inner-ring iodine atom of T4 AM forms a halogen bond with the $MeSe^-$ ion with an interaction energy of 62.89 kcal mol^{-1}, which is higher than that observed for T3 AM. Therefore, it is expected that T4 AM should undergo inner-ring deiodination readily by **3**. When T4 AM was added to the assay mixture, the solution became turbid, thus indicating that the solubility of T4 AM in 20% (v/v) acetonitrile and phosphate buffer is lower than that of T4 and T3 AM. When the deiodination reaction was carried out in 100% acetonitrile, T4 AM underwent deiodination by **3** to produce rT3 AM, T3 AM, and a small of amount of 3,3′-T2 AM (see Figure S22 in the Supporting Information). These observations indicate that the solvent has a remarkable effect in deiodination reactions.

Our earlier reports showed that the introduction of a secondary-amine moiety in proximity to one of the selenol groups in **3** led to increase in deiodinase activity relative to **3**. Herein, we report the effect of the sulfur-containing thioacetal moiety **4** (Figure 4a) in proximity to one of the selenol groups in **3**. Compound **4** was freshly prepared by reducing the corresponding diselenide **5** (Figure 4b) with sodium borohydride. Interestingly, **4** was 1.8- and 2.3-fold more active than **3** in the deiodination of T3 to 3,3′-T2 and T3 AM to 3,3′-T2 AM (Figure 5). With the help of a lone pair of electrons, the sulfur atoms of the thioacetal moiety in **4**, may interact with the proximal selenol group during the reaction. As co-operative halogen and chalcogen bonding is important for deiodination, the donation of electron density by the sulfur atoms further strengthens the chalcogen bonding, and hence halogen bonding, thus facilitating the deiodination reactions. Single-crystal X-ray studies of **5** indicate that one of the sulfur atoms interacts with the selenium atom, which is similar to the Se···N interactions in the secondary-amine-substituted deiodinase mimics reported earlier (Figure 4b).[12] The presence of the noncovalent Se···S interaction in **4** can be understood from the chemical shifts in the ^{77}Se NMR spectra (Figure 4c). The signal for the selenol group adjacent to the sulfur moiety in **4** ($\delta =$ 102 ppm) is significantly shifted upfield relative to the other selenol group ($\delta = 205$ ppm) in the same compound or **3** ($\delta =$ 156 ppm). These results indicate a more nucleophilic character of the selenol group adjacent to the sulfur atom of the thioacetal moiety relative to the other selenol group.

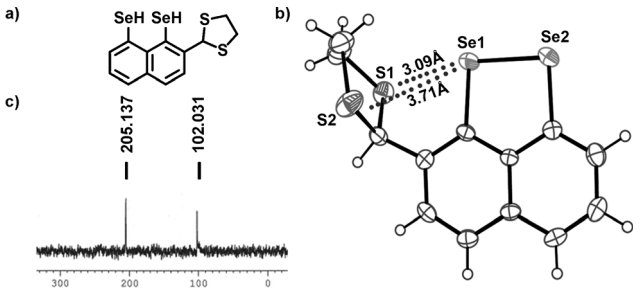

Figure 4. a) Chemical structure of **4**. b) ORTEP diagram of a single-crystal X-ray structure of **5**, indicating Se···S noncovalent interactions. The thermal ellipsoids are drawn at 30% probability. c) ^{77}Se NMR spectrum of **4** in chloroform/methanol (1:1). Chemical-shift values [ppm] are cited with respect to $(CH_3)_2Se$ as an external standard.

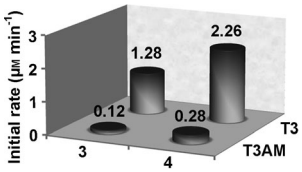

Figure 5. Initial rates of deiodination of T3 and T3 AM by **3** and **4** under identical conditions. Assay conditions: T3 or T3 AM (0.3 mM), mimic (1.2 mM), DTT (15 mM), $NaBH_4$ (30 mM), phosphate buffer (100 mM, pH 7.00), 20% (v/v) acetonitrile, 37 °C.

Interestingly, the initial rates of deiodination of T3 AM by **3** and **4** are almost 11- and 8-fold, respectively, less than that of T3 (Figure 5), thus indicating that the removal of the carboxyl group from the β-alanine side chain of T3 decreases the rate of deiodination without affecting the regioselectivity. This outcome is in agreement with the report of Köhrle and co-workers that the rates of outer- and inner-ring deiodination of iodothyronamines by deiodinases are lower than that of thyroid hormones.[5] To understand the difference in the reactivity of the iodine atoms in T3 and T3 AM, we carried out DFT calculations on T3 and T3 AM with the $MeSe^-$ ion. The Se···I distance for the outer-ring iodine atom in T3 (3.018 Å) is slightly shorter than that in T3 AM (3.024 Å). In contrast, the Se···I distance for the inner-ring iodine atom in T3 (2.942 Å) is significantly shorter than that in T3 AM (2.955 Å; Figures 3 and 6). As a result, the inner-ring C–I bond in T3 is more elongated (2.338 Å) relative to T3 AM (2.326 Å). Consequently, the energies for the noncovalent interactions between the $MeSe^-$ ion and the inner-ring iodine atom is 62.58 and 59.03 kcal mol^{-1} for T3 and T3 AM, re-

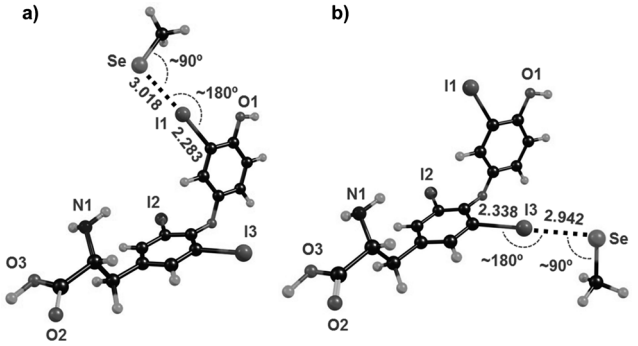

Figure 6. A comparison of the Se···I distances, C–I bond lengths [Å], and C-I-Se and C-Se-I angles [°] for the a) outer-ring and b) inner-ring iodine atoms in the halogen-bonded adducts of T3 with the $MeSe^-$ ion.

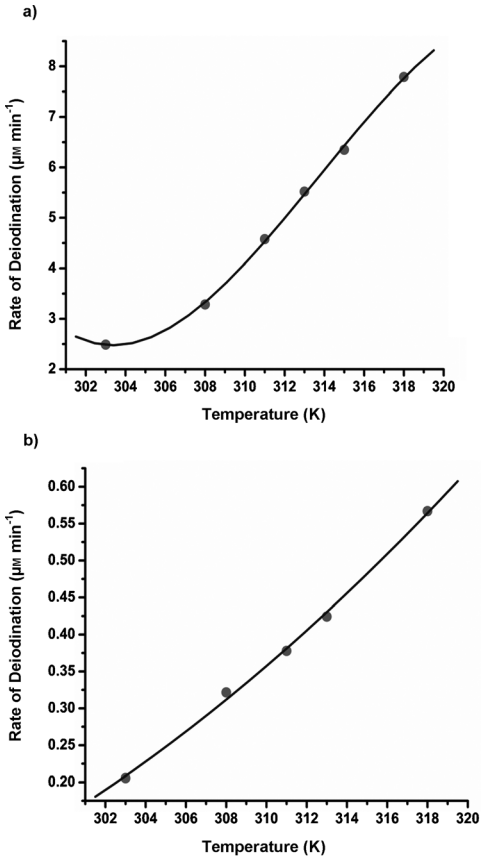

Figure 7. Effect of temperature on the initial rate of deiodination of a) T3 and b) T3 AM by **4**. Assay conditions: T3 or T3 AM (0.3 mM), **4** (1.2 mM), DTT (15 mM), $NaBH_4$ (30 mM), phosphate buffer (100 mM, pH 7), and 20% (v/v) acetonitrile.

spectively. Therefore, the inner-ring deiodination of T3 by the selenium compounds is expected to be faster than that of T3 AM. However, the marginal difference in the halogen-bond energy may not be sufficient to explain the 7–11-fold increase in the rate of deiodination of T3. To this end, we carried out detailed kinetic experiments.

To understand the differences in the rate of deiodination of T3 and T3 AM, we determined the activation-energy barrier for the reactions from Arrhenius plots (see below).[13] Briefly, the effect of temperature on the deiodination of T3 and T3 AM by **4** was studied over a temperature range of 303–318 K at pH 7.[14] These experiments indicate that the rate of deiodination of T3 and T3 AM increases with temperature (Figure 7). Interestingly, there was no change in regioselectivity up to 318 K.

As none of the intermediates in the deiodination reaction is isolable, an overall rate constant instead of the rate constant for the rate-determining step may be used. For this purpose, we determined the order of the deiodination reactions.[15] Detailed kinetic experiments indicate that deiodination of T3 is overall a third-order reaction, that is, second order with respect to T3 and first order with respect to **4**. In contrast, deiodination of T3 AM is overall a second-order reaction, that is, first order with respect to T3 AM and first order with respect to **4** (Figure 8a,b). From the Arrhenius plot, the activation energies for the deiodination of T3 and T3 AM is calculated to be 63.6 and 53.3 kJ mol^{-1}, respectively (Figure 9). These observations suggest that the rate of deiodination of T3 should be lower than that of T3 AM. However, the collision frequency or pre-exponential factor[16] for T3 is two-fold higher (1.99×10^3) than for T3 AM (0.89×10^3). Structural preorganisation of T3 in solution is probably responsible for the facile and effective attack of the selenol moiety in **4** on the T3 iodine atoms (see below).

As discussed earlier, the deiodination of T3 is second order with respect to T3, whereas the deiodination of T3 AM is first order with respect to T3 AM, although both the deiodination reactions are first order with respect to diselenol **4**. Therefore, in the two independent reactions, one molecule of **4** may interact with two molecules of T3 or one molecule of T3 AM, respectively.[17] Alternatively, T3 molecules may interact noncovalently with each other to form a dimeric species before the reaction with **4**. In such case, a decrease in the concentration of T3, that is, an increase in the molecular separation, should lead to the formation of a monomeric T3 species in solution. To understand the effect of concentration on the intermolecular interactions, we carried out UV/Vis spectroscopic experiments at different concentrations of T3 and T3 AM. The UV/Vis spectra of T3 (at 0.5 mM concentration), showed $\lambda_{max}=322$ nm and a small hump at around $\lambda=289$ nm (Figure 10a). When the concentration was decreased, the λ_{max} value remained unchanged up to 0.2 mM. A further decrease in the concentration of T3 shifted the λ_{max} value to a lower wavelength ($\lambda_{max}=$ 296 nm). Interestingly, at lower concentrations, T3 exhibited a shoulder at around $\lambda=322$ nm, which gradually disappeared upon further dilution, thus indicating the presence of two species in equilibrium with each other. The species that exhibits $\lambda_{max}=322$ nm appears to be the T3 dimer, whereas the T3 monomer exhibits $\lambda_{max}=296$ nm. In contrast, the absorption spectra of T3 AM (Figure 10b) shows only one peak at $\lambda=296$ nm over a wide concentration range of 0.05–0.5 mM, thus indicating the presence of only the monomeric species.

As the concentration of T3 (0.3 mM) used for the deiodinase assays is identical to the concentration that helps the formation of a dimer species, the reaction of selenol is expected to occur with the dimeric form of T3. This behaviour is consistent

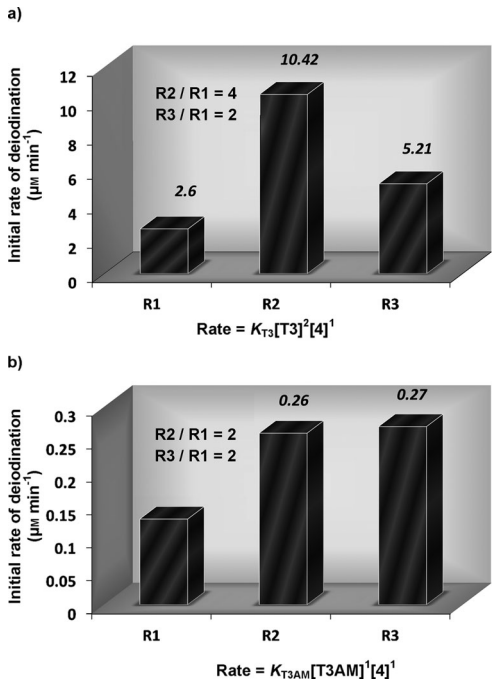

Figure 8. Determination of the order of the deiodination reactions of a) T3 and b) T3AM by **4**. R1: initial rate for T3 or T3AM (0.3 mM); R2: initial rate for T3 or T3AM (0.6 mM); R3: initial rate for T3 or T3AM (0.3 mM). Although the concentration of **4** used for determining R1 and R2 was 0.3 mM, it was 0.6 mM for R3. K_{T3} and K_{T3AM}: the rate constant for the deiodination reactions of T3 and T3AM, respectively. The concentrations of DTT and $NaBH_4$ used were 15 and 7.5 mM, respectively. The reactions were carried out in phosphate buffer (100 mM, pH 7) and 20% (v/v) acetonitrile at 37 °C.

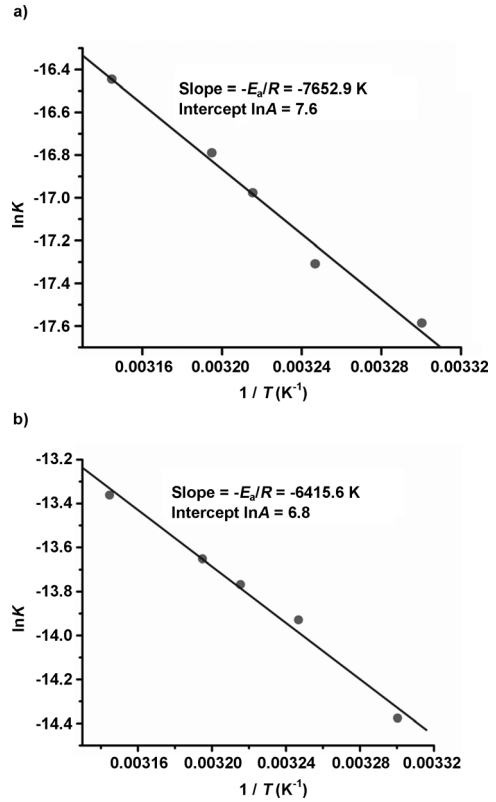

Figure 9. Arrhenius plots for the deiodination of a) T3 and b) T3AM by **4**.

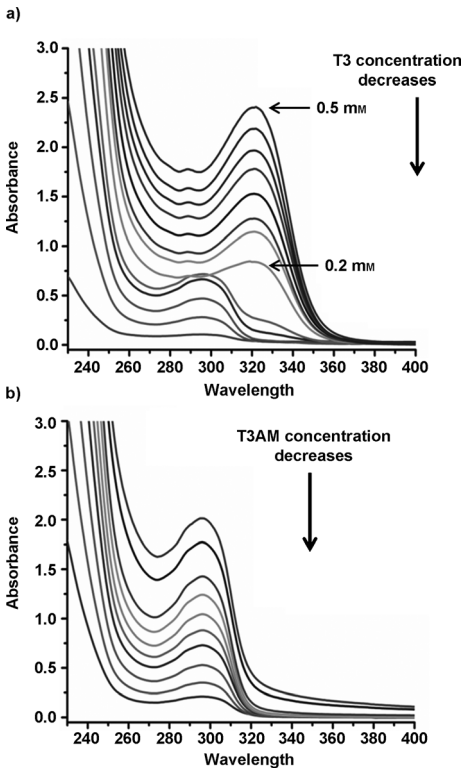

Figure 10. Concentration-dependent UV/Vis absorption spectra of a) T3 and b) T3AM. The spectra of T3 and T3AM were recorded in 20% (v/v) acetonitrile in phosphate buffer (100 mM, pH 7.0).

with the results of the kinetic experiments, which show that the deiodination reaction is second order with respect to T3. On the other hand, the reaction between T3AM and the selenol group should occur with the monomeric form of T3AM because no dimer formation was observed up to the concentration of 0.5 mM. Therefore, the deiodination reaction is first-order with respect to T3AM (see above). Interestingly, when the kinetic experiments were carried out for the deiodination reaction at 0.08 mM concentration, the reaction was first order with respect to T3 when T3 exists only as a monomeric species (see Figure S23 in the Supporting Information), thus indicating that the intermolecular interactions in solution have a significant effect on the deiodination kinetics.

To understand the intermolecular interactions in T3 and T3AM further, we determined the single-crystal X-ray structures of these two compounds. The crystal structure of T3 indicates the presence of closely packed layers with extensive hydrogen bonding with trifluoroacetate ions and water (Figure 11a). The carboxyl group in the β-alanine side chain in one molecule forms water-mediated hydrogen bonding with the 4′-OH group of the neighbouring molecule. Interestingly, the two inner-ring iodine atoms interact with the inner-ring iodine atoms of the neighbouring molecule, and each iodine atom forms a bifurcated halogen bond. The I···I distances of 3.86 and 3.64 Å are shorter than the sum of the van der Waals radii (3.96 Å). However, the outer-ring iodine atom is not involved in I···I halogen bonding. These observations indicate that the inner-ring iodine atoms in T3 are more susceptible to halogen

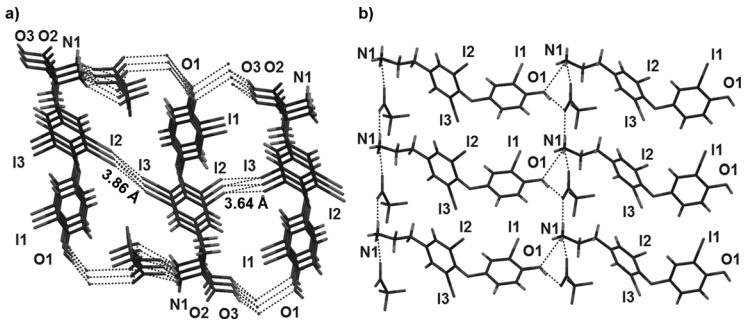

Figure 11. Single-crystal X-ray structures that indicate a) intermolecular hydrogen and halogen bonding in T3 and b) hydrogen bonding in T3 AM.

bonding than the outer-ring iodine atom. Similar to T3, the crystal packing of T3 AM also indicates the presence of hydrogen bonding between the 4′-OH group, protonated amine group, and the trifluoroacetate carboxylate ion (Figure 11 b). However, no I···I interactions were observed in T3 AM, thus indicating that the iodine atoms in this compound do not favour halogen bonding.

As some of the intermolecular interactions found in the crystal structure may break down in solution and the kinetic data support the formation of a dimer in solution, we presume that a dimeric form is responsible for the observed reactivity of T3. It has been shown that the dimeric form of T3 favours the attack of the selenol group on the inner-ring iodine atom of T3. Therefore, along with hydrogen bonding, I···I halogen bonding may take part in the formation of dimeric species of T3 in solution. Previously, halogen bonding in solution has been reported for the formation of supramolecular gels, transmembrane transport of anions, anion recognition and coordination, and the design of efficient inhibitors of enzymes.[18] The halogen–halogen (Br···Br and I···I) interaction in solution is also known to be an important factor for the assembly of crystalline nanoparticles in aqueous suspension by both 3-bromo- and 3-iodocarbazoles.[19] Therefore, to understand the effect of I···I interactions on the reactivity of an inner-ring iodine atom, we carried out DFT calculations on the dimeric form by using the coordinates obtained from X-ray data (after removing the trifluoroacetate ion and water). The two T3 molecules, in which the iodine atoms interact with each other with an I···I distance of 3.64 Å (Figure 12 a), were considered for the calculations. The NBO analysis indicates that the inner-ring iodine atoms in individual T3 molecules have similar charges (0.260 a.u.). However, upon interaction with each other, the charge on I_A becomes significantly more positive than on I_B (0.276 versus 0.217 a.u., respectively). These observations indicate that one iodine atom acts as an electron donor (halogen-bond acceptor), whereas the other iodine atom acts as an electron acceptor (halogen-bond donor). The iodine atom that carries more positive charge is expected to form a stronger halogen bond with a selenium atom (in the selenol group) than the one that has a less positive charge (Figure 12 b). Thus, intermolecular I···I halogen bonding may facilitate the attack of the selenol group on T3 relative to T3 AM.

It is known that one or more histidine (His) residues in the active site of ID-1 plays an important role in the deiodination reaction of thyroid hormones in addition to the cysteine (Cys) and Sec (selenocysteine) residues. Köhrle and others have shown an enhancement in nucleophilicity of the Sec residue in the active site of ID-1 by the formation of an imidazolium–selenolate ion pair.[20] His residues at the 158 and 174 positions in human ID-1 are conserved in ID-2 and ID-3, although the formation of the imidazolium–selenolate ion pair has not been proposed for ID-3.[2a] Goto et al. reported that the outer-ring deiodination of *N*-butyrylthyroxine methyl ester by a steri-

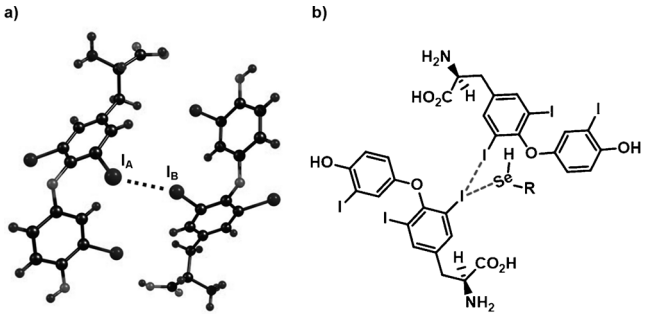

Figure 12. a) Structure of I···I halogen-bonded dimer of T3 for NBO analysis. b) Possible mode of interaction of the T3 dimer with a selenol group.

cally hindered selenol group takes place only in the presence of triethylamine.[21] This outcome has been explained by the increase in the nucleophilicity of the selenol group by trimethylamine. We also noticed that the inner-ring deiodination of T3 or T3 AM can be enhanced by adding trimethylamine to the reaction mixture. The NBO analysis indicates that the positive potential (0.207 a.u.) on the inner-ring iodine atoms of T3 is increased with halogen bonding to trimethylamine (0.217 a.u.). Furthermore, the C—I bond of the inner-ring iodine atom in T3 (2.127 Å) is significantly elongated in the presence of trimethylamine (2.139 Å). The electron density, donated by the halogen-bond acceptor triethylamine, becomes delocalised on the phenyl ring and makes the iodine atom more susceptible towards deiodination. These observations indicate that any halogen-bond acceptor can polarise the C—I bond.

Conclusion

The regioselective deiodination of iodothyronamines by synthetic deiodinase mimics has been described. A sulfur atom in proximity to a selenol group in naphthyl-based compounds enhances the deiodinase activity. The rate of deiodination of 3,3′,5-triiodothyronine (T3) was 8–11-fold higher than that of 3,3′,5-triiodothyronamine (T3 AM). Detailed kinetic experiments indicate that the deiodination reactions of T3 and T3 AM are second order with respect to T3 and first order with respect to T3 AM. However, the order of the reaction depends on the concentration of T3 because the reaction is first order with respect

to T3 at lower concentrations, thus indicating that intermolecular interactions play an important role in deiodination. Single-crystal X-ray studies of T3 indicated the presence of novel I···I halogen bonds, which are absent in the crystal structure of T3 AM. These observations suggest that not only the halogen bond between the iodine and selenium atoms, but also I···I intermolecular interactions, facilitate deiodination of thyroid hormones.

Experimental Section

General procedure

Tyramine, iodine monochloride (ICl), triisopropylborate, tetrabutylammonium fluoride (TBAF), borontrifluoride diethyletherate ($BF_3{\cdot}Et_2O$), ethanedithiol, selenium powder, T4, rT3, T3, and acetonitrile were purchased from Sigma–Aldrich. *n*-Butyllithium (*n*BuLi) was obtained from Acros Chemical Co. (Belgium). Dithiothreitol (DTT) and anhydrous cupric acetate were obtained from Alfa Aesar. Trifluoroacetic acid (TFA) and precoated silica-gel plates were purchased from Merck. Liquid-state NMR spectra were recorded in $CDCl_3$, [D_4]MeOH, or [D_6]DMSO as a solvent. ^{1}H, ^{13}C, and ^{77}Se NMR spectra were obtained using a Bruker 400 MHz NMR spectrometer (400, 100.56, 76.29 MHz, respectively). Chemical-shift values are cited with respect to $SiMe_4$ as an internal (^{1}H and ^{13}C) and Me_2Se as an external (^{77}Se) standard. Column chromatography was carried out in glass columns or in an automated flash-chromatography system (Biotage) by using preloaded silica cartridges. HPLC experiments were performed on a Waters Alliance system (Milford, MA, USA) consisting of a 2695 separation module and a 2996 photodiode-array detector. HPLC sample vials (1.7 mL) were used to carry out the deiodinase assays, and a built-in auto-sampler was used for sample injection. The HPLC system was controlled by EMPOWER software (Waters corporation, Milford, MA, USA). Single-crystal X-ray diffraction data were obtained from a Bruker Kappa Apex II X-ray diffractometer with a CCD detector. Compounds **20** and **21** were synthesised by following a reported procedure.[7,9]

Deiodination assays

The deiodination reactions of thyroid hormones and iodothyronamines were carried out in a mixture of 20% (v/v) acetonitrile and phosphate buffer (100 mM, pH 7.00) at 37 °C in the presence of 15 mM DTT. Acetonitrile was used to increase the solubility of iodothyronamines in phosphate buffer at physiological pH values. The selenol compounds (1.2 mM) were freshly prepared by reducing the corresponding diselenide with sodium borohydride. To determine the initial rate of deiodination, the deiodination of thyroid hormones or iodothyronamines (0.3 mM) was followed during the initial period (ca. 10%) of the reaction. The deiodinated products were analysed by using reverse-phase HPLC (Princeton C18 column; 150×5 mm, I.D. = 5 μm) with gradient elution and acetonitrile/ammonium acetate/acetic acid buffer (15 mM, pH 4) as the mobile phase. The formation of deiodinated products was monitored at $\lambda = 275$ nm, and the yields of their formation were calculated from the corresponding peak areas.

Synthesis

Synthesis of 5: 1,2-Ethanedithiol (46 mg, 0.49 mmol) was added to a solution of **21** (100 mg, 0.32 mmol) in dry dichloromethane (20 mL). The resulting solution was cooled to 0 °C. Borontrifluoride diethyl etherate (80 μL, 45–50% solution) was added dropwise to the mixture at 0 °C, which was warmed to room temperature over 12 h. The mixture was diluted with excess dichloromethane, washed with water (5×), dried over anhydrous sodium sulfate, and evaporated under reduced pressure to give a dark-brown liquid. The crude product was purified by column chromatography with petroleum ether/diethyl ether as the eluent to give **5** as a dark-brown solid in 35% yield. ^{1}H NMR ($CDCl_3$): $\delta = 7.51$ (d, $J = 8.4$ Hz, 1H), 7.44 (t, $J = 6.8$ Hz, 2H), 7.33 (d, $J = 8$ Hz, 1H), 7.24–7.28 (q, $J = 5.6$ Hz, 1H), 5.87 (s, 1H), 3.61–3.67 (m, 2H), 3.41–3.45 ppm (m, 2H); ^{13}C NMR ($CDCl_3$): $\delta = 141.4$, 141.3, 139.7, 137.6, 132.9, 129.1, 128.0, 125.2, 123.6, 122.8, 58.9, 41.0 ppm; ^{77}Se NMR ($CDCl_3$): $\delta = 453$, 382 ppm.

Synthesis of T4 AM: *N-tert*-butoxycarbonyl-3,3′,5,5′-tetraiodothyronamine (200 mg, 0.24 mmol) was stirred in 1:4 (v/v) mixture of trifluoroacetic acid and dichloromethane for 1 h. The solvent was evaporated under vacuum to yield a yellow–white sticky solid. T4 AM was purified from the crude reaction mixture by using a reverse-phase HPLC with a C18 column (Atlantis; 250×19 mm, I.D. = 10 μm) and methanol/water (70:30) as the mobile phase. T4 AM-containing fractions were lyophilised to yield a white solid in 90% yield. ^{1}H NMR ([D_4]MeOH): $\delta = 7.89$ (s, 2H), 7.10 (s, 2H), 3.22 (t, $J = 7.6$ Hz, 2H), 2.94 ppm (t, $J = 7.6$ Hz, 2H); ^{13}C NMR ([D_4]MeOH): $\delta = 153.3$, 151.6, 150.7, 141.0, 138.6, 126.2, 91.1, 84.7, 40.4, 31.8 ppm; MS (ESI): *m/z* calcd for $C_{14}H_{11}NO_2I_4$: 733.7 ($[M+H]^+$); found 734.06.

Synthesis of T3 AM: This compound was synthesised by using *N-tert*-butoxycarbonyl-3,3′,5-triiodothyronamine (200 mg, 0.28 mmol) as described earlier for T4 AM in 92% yield. ^{1}H NMR ([D_4]MeOH): $\delta = 7.89$ (s, 2H), 7.00 (d, $J = 2.8$ Hz, 1H), 6.78 (d, $J = 8.8$ Hz, 1H), 6.64–6.67 (dd, $J = 6.4$ Hz, 1H), 3.23 (t, $J = 8$ Hz, 2H), 2.95 (t, $J = 7.2$ Hz, 2H); ^{13}C NMR ([D_4]MeOH): $\delta = 153.9$, 152.5, 149.9, 141.0, 138.2, 125.6, 116.8, 115.0, 91.4, 83.4, 40.5, 31.8; MS (ESI): *m/z* calcd for $C_{14}H_{13}NO_2I_3$: 607.81 ($[M+H]^+$); found: 607.77.

Synthesis of rT3 AM: This compound was synthesised by using *N-tert*-butoxycarbonyl-3,3′,5′-triiodothyronamine (200 mg, 0.28 mmol) as described earlier for T4 AM in 95% yield. ^{1}H NMR [D_4]MeOH): $\delta = 7.85$ (s, 1H), 7.31 (s, 3H), 6.91 (d, $J = 8.4$ Hz, 1H), 4.64 (br, s, 2H), 3.19 (t, $J = 7.6$ Hz, 2H), 2.9 ppm (t, $J = 7.6$ Hz, 2H); ^{13}C NMR ([D_4]MeOH): $\delta = 156.0$, 152.6, 151.3, 140.5, 135.0, 130.7, 129.0, 119.8, 88.8, 84.5, 40.7, 32.3 ppm; MS (ESI): *m/z* calcd for $C_{14}H_{13}NO_2I_3$: 607.81 ($[M+H]^+$); found: 607.71.

Synthesis of 3,3′-T2 AM: This compound was synthesised by using *N-tert*-butoxycarbonyl-3,3′-diiodothyronamine (200 mg, 0.34 mmol) as described earlier for T4 AM in 93% yield. ^{1}H NMR ([D_4]MeOH): $\delta = 7.81$ (d, $J = 2$ Hz, 1H), 7.22–7.24 (q, $J = 4$ Hz, 2H), 6.84 (t, $J = 2.8$ Hz, 1H), 6.78 (d, $J = 8.4$ Hz, 1H), 3.16 (t, $J = 8$ Hz, 2H), 2.91 ppm (t, $J = 7.6$ Hz, 2H); ^{13}C NMR ([D_4]MeOH): $\delta = 157.0$, 153.9, 149.9, 140.3, 133.9, 130.4, 129.4, 120.2, 118.5, 115.1, 88.0, 83.4, 40.8, 32.3 ppm; MS (ESI): *m/z* calcd for $C_{14}H_{14}NO_2I_2$: 481.91 ($[M+H]^+$); found: 481.85.

Single-crystal X-ray crystallography

Compound **5** was recrystallised from chloroform by using the slow-evaporation method. Dark-brown crystals were filtered, washed with petroleum ether, and dried under high vacuum. T3 was recrystallised with trifluoroacetic acid from a solution of diethyl ether and ethyl acetate (1:1). The needle-shaped white crystals obtained from the solution were dried under vacuum. T3 AM was also recrystallised as a trifluoroacetate salt by following a similar procedure. The single-crystal X-ray diffraction data of **5**, T3, and T3 AM were collected on a Bruker SMART APEX CCD diffractometer by utilizing SMART/SAINT software.[22] Intensity data were collected by using graphite-monochromatised MoKα radiation of wave-

length 0.71073 Å at room temperature. All the structures were solved by using the SHELX-97 program incorporated in WinGX. Empirical absorption corrections were applied with SADABS.[23,24] All the non-hydrogen atoms were refined by anisotropic-displacement coefficients except one carbon atom (C10) in the phenolic ring of T3. The hydrogen atoms on the carbon, nitrogen, and oxygen atoms were included in geometric positions and given thermal parameters are equivalent to 1.2× the atoms to which they were attached.

Crystal data for 5: $C_{13}H_{10}S_2Se_2$, $M_r = 388.27$, monoclinic, $P2_1/c$, $a = 12.0408(13)$, $b = 11.0451(11)$, $c = 10.3597(11)$ Å; $\alpha = 90$, $\beta = 112.223(3)$, $\gamma = 90°$; $V = 1275.4(2)$ Å^3, $Z = 4$, MoKα radiation ($\lambda = 0.71073$ Å), $T = 273(2)$ K, $\rho_{calcd} = 2.022$ g cm^{-3}, μ(MoKα) = 6.097 mm^{-1}; collected reflections = 2978, unique reflections = 2138, GOF (F^2) = 1.041, R_1[a] = 0.0441, wR_2[b] = 0.1045.

Crystal data for T3·CF_3CO_2: $C_{17}H_{13}NO_8F_3I_3$, $M_r = 796.98$, monoclinic, $P2_1$, $a = 15.124(3)$, $b = 5.0451(10)$, $c = 16.052(3)$ Å; $\alpha = 90$, $\beta = 103.409(12)$, $\gamma = 90°$; $V = 1191.5(4)$ Å^3, $Z = 2$, MoKα radiation ($\lambda = 0.71073$ Å), $T = 296(2)$ K, $\rho_{calcd} = 2.222$ g cm^{-3}, μ(MoKα) = 4.000 mm^{-1}; collected reflections = 7017, unique reflections = 3357, GOF (F^2) = 0.957, R_1[a] = 0.0578, wR_2[b] = 0.1373.

Crystal data for T3 AM·CF_3CO_2: $C_{16}H_{13}NO_4F_3I_3$, $M_r = 720.97$, monoclinic, $P2_1/C$, $a = 6.565(4)$, $b = 11.892(8)$, $c = 27.565(18)$ Å; $\alpha = 90$, $\beta = 89.92(4)$, $\gamma = 90°$; $V = 2152(2)$ Å^3, $Z = 4$, MoKα radiation ($\lambda = 0.71073$ Å), $T = 296(2)$ K, $\rho_{calcd} = 2.225$ g cm^{-3}, μ(MoKα) = 4.403 mm^{-1}; collected reflections = 5070, unique reflections = 1967, GOF (F^2) = 0.901, R_1[a] = 0.0732, wR_2[b] = 0. 2089.

[a] $R1 = \Sigma||F_o| - |F_c||/\Sigma|F_o|$. [b] $wR_2 = \{\Sigma[w(F_o^2 - F_c^2)^2]/\Sigma[w(F_o^2)^2]\}^{1/2}$.

Computational methods

All the DFT calculations were performed by using the Gaussian03 and Gaussian09 suites of quantum-chemical programs.[25] The hybrid Becke 3-Lee–Yang–Parr (B3LYP) exchange correlation functional was used to predict the molecular geometries with minimum energy.[26] All the hormones and hormone metabolites were optimised at the B3LYP level using 6–31 + G* basis sets for all the atoms, except iodine for which the 6–311G** basis set was used. Frequency calculations were performed for each optimised geometry at the same level of theory by using the same basis sets to ensure that there was a minimum on the potential-energy surface. NBO calculations[27] were performed by using 6–311 + G** basis sets, except iodine for which the 6–311G** basis set was used.

Acknowledgements

This study was supported by the Department of Science and Technology (DST), New Delhi. G.M. acknowledges the DST for the award of a Swarnajayanti Fellowship, and S.M. thanks the Indian Institute of Science for a research fellowship.

Keywords: enzyme models · hormones · iodine · noncovalent interactions · selenium

[1] a) D. Behne, A. Kyriakopoulos, H. Meinhold, J. Köhrle, *Biochem. Biophys. Res. Commun.* **1990**, *173*, 1143–1149; b) J. L. Leonard, T. J. Visser in *Biochemistry of Deiodination in Thyroid Hormone Metabolism* (Ed.: G. Hennemann), Marcel Dekker, New York, **1986**, p. 189; c) M. J. Berry, L. Banu, P. R. Larsen, *Nature* **1991**, *349*, 438–440; d) P. R. Larsen, M. J. Berry, *Annu. Rev. Nutr.* **1995**, *15*, 323; e) J. L. Leonard, J. Köhrle in *Intracellular Pathways of Iodothyronine Metabolism in The Thyroid* (Eds.: L. E. Braverman, R. D. Utiger), Lippincott-Raven, Philadelphia, **1996**, p. 144; f) D. L. St. Germain, V. A. Galton, *Thyroid* **1997**, *7*, 655–668.

[2] a) A. C. Bianco, D. Salvatore, B. Gereben, M. J. Berry, P. R. Larsen, *Endocr. Rev.* **2002**, *23*, 38–89; b) J. Köhrle, *Methods Enzymol.* **2002**, *347*, 125–167; c) G. G. J. M. Kuiper, M. H. A. Kester, R. P. Peeters, T. J. Visser, *Thyroid* **2005**, *15*, 787–798.

[3] a) T. J. Visser, C. H. H. Schoenmakers, *Acta Med. Austriaca* **1992**, *19*, 18–21; b) J. Köhrle, *Mol. Cell. Endocrinol.* **1999**, *151*, 103–119; c) J. Köhrle, F. Jakob, B. Contempré, J. E. Dumont, *Endocr. Rev.* **2005**, *26*, 944–984.

[4] a) T. S. Scanlan, K. L. Suchland, M. E. Hart, G. Chiellini, Y. Huang, P. J. Kruzich, S. Frascarelli, D. A. Crossley II, J. R. Bunzow, S. Ronca-Testoni, E. T. Lin, D. Hatton, R. Zucchi, D. K. Grandy, *Nat. Med.* **2004**, *10*, 638–642; b) K. P. Doyle, K. L. Suchland, T. M. P. Ciesielski, N. S. Lessov, D. K. Grandy, T. S. Scanlan, M. P. Stenzel-poore, *Stroke* **2007**, *38*, 2569–2576.

[5] S. Piehl, T. Heberer, G. Balizs, T. S. Scanlan, R. Smits, B. Koksch, J. Köhrle, *Endocrinol.* **2008**, *149*, 3037–3045.

[6] D. Manna, G. Mugesh, *Angew. Chem.* **2010**, *122*, 9432–9435; *Angew. Chem. Int. Ed.* **2010**, *49*, 9246–9249.

[7] D. Manna, G. Mugesh, *J. Am. Chem. Soc.* **2011**, *133*, 9980–9983.

[8] M. E. Hart, K. L. Suchland, M. Miyakawa, J. R. Bunzow, D. K. Grandy, T. S. Scanlan, *J. Med. Chem.* **2006**, *49*, 1101–1112.

[9] D. Manna, G. Mugesh, *J. Am. Chem. Soc.* **2012**, *134*, 4269–4279.

[10] P. Metrangolo, F. Meyer, T. Pilati, G. Resnati, G. Terraneo, *Angew. Chem.* **2008**, *120*, 6206–6220; *Angew. Chem. Int. Ed.* **2008**, *47*, 6114–6127.

[11] P. Auffinger, F. A. Hays, E. Westhof, P. S. Ho, *Proc. Natl. Acad. Sci. USA* **2004**, *101*, 16789–16794.

[12] CCDC-992507 (T3), -992508 (T3 AM), -992509 (**5**) contain the supplementary crystallographic data for this paper. These data can be obtained free of charge from The Cambridge Crystallographic Data Centre via www.ccdc.cam.ac.uk/data_request/cif.

[13] To understand the kinetics of the deiodination of T3 and T3 AM, the activation energy was determined from the Arrhenius equation: $\ln K = \ln A - E_a/RT$ (K is the rate constant; A is the pre-exponential factor, which indicates the frequency of collisions between reactants; E_a is the activation energy; R is the universal gas constant; and T is the temperature in K); a plot of $\ln K$ versus $1/T$ is expected to produce a straight line with a negative slope of magnitude E_a/R and an intercept $\ln A$; a) R. D. Levine, in *Molecular Reaction Dynamics*, Cambridge University Press, **2005**; b) K. J. Laidler, in *Chemical Kinetics*, Third Edition, Harper & Row, New York, **1987**, p. 42.

[14] For calculating the rate constants (K), the initial rate of deiodination was determined at different temperatures in the range 303–318 K.

[15] For a bimolecular reaction between A and B, the rate of reaction (R) = $K[A]^{n1}[B]^{n2}$, where $n1$ and $n2$ are the orders of reaction with respect to A and B, respectively; therefore, to determine the rate constant from the rate of deiodination, it is necessary to know the order of the deiodination reactions; the order of deiodination reactions was determined by following a procedure shown in Scheme S03 in the Supporting Information: a) R. H. Petrucci, W. S. Harwood, F. G. Herring in *General Chemistry*, 8edth edPrentice-Hall, **2002**, p. 585–586; b) P. Atkins, J. D. Paula in *Physical Chemistry*, 8edth ed W. H. Freeman and Company, New York, **2006**, p. 797–798.

[16] a) R. Chang in *Physical Chemistry for the Biosciences*, University Science Books, Sausalito, CA, **2005**; b) P. Atkins, J. D. Paula in *Physical Chemistry for the Life Sciences*, Alexandria, VA, **2006**.

[17] Probability of obtaining three reactant molecules (two molecules of T3 and one molecule of selenol) in suitable orientations for effective collision is expected to be less than bringing together two reactant molecules (one molecule of T3 AM and one molecule of selenol); as the third-order deiodination reaction of T3 is expected to be slower than the deiodination of T3 AM, the reaction of one molecule of selenol with two separate molecules of T3 may be excluded.

[18] a) L. Meazza, J. A. Foster, K. Fucke, P. Metrangolo, G. Resnati, J. W. Steed, *Nat. Chem.* **2012**, *5*, 42–47; b) A. Vargas Jentzsch, D. Emery, J. Mareda, S. K. Nayak, P. Metrangolo, G. Resnati, N. Sakai, S. Matile, *Nat. Commun.* **2012**, *3*, 905; c) G. Cavallo, P. Metrangolo, T. Pilati, G. Resnati, M. Sansotera, G. Terraneo, *Chem. Soc. Rev.* **2010**, *39*, 3772–3783; d) O. El-Kabbani, D. A. Carper, M. H. McGowan, Y. Devedjiev, K. J. Rees-Milton, T. G. Flynn, *Proteins* **1997**, *29*, 186–192; e) E. I. Howard, R. Sanishvili, R. E. Cachau, A. Mitschler, B. Chevrier, P. Barth, V. Lamour, M. Van Zandt, E. Sibley, C. Bon, D. Moras, T. R. Schneider, A. Joachimiak, A. Podjarny, *Proteins* **2004**, *55*,

792 – 804; f) R. Wilcken, X. Liu, M. O. Zimmermann, T. J. Rutherford, A. R. Fersht, A. C. Joerger, F. M. Boeckler, *J. Am. Chem. Soc.* **2012**, *134*, 6810 – 6818; g) D. M. Himmel, K. Das, A. D. Clark, J. S. H. Hughes, A. Benjahad, S. Oumouch, J. Guillemont, S. Coupa, A. Poncelet, I. Csoka, C. Meyer, K. Andries, C. H. Nguyen, D. S. Grierson, E. Arnold, *J. Med. Chem.* **2005**, *48*, 7582 – 7591.

[19] W. J. Liang, Y. Wang, F. Feng, W. J. Jin, *Anal. Chim. Acta* **2006**, *572*, 295 – 302.

[20] a) J. Köhrle, R. D. Hesch, *Horm. Metab. Res. Suppl.* **1984**, *14*, 42 – 55; b) M. J. Berry, *J. Biol. Chem.* **1992**, *267*, 18055 – 18059.

[21] K. Goto, D. Sonoda, K. Shimada, S. Sase, T. Kawashima, *Angew. Chem.* **2010**, *122*, 555 – 557; *Angew. Chem. Int. Ed.* **2010**, *49*, 545 – 547.

[22] A. Altomare, G. Cascarano, C. Giacovazzo, A. Gualardi, *J. Appl. Crystallogr.* **1993**, *26*, 343 – 350.

[23] G. M. Sheldrick, *Acta Crystallogr. Sect. A* **1990**, *46*, 467 – 473.

[24] G. M. Sheldrick, SHELX-97, Program for the Refinement of Crystal Structures; University of Göttingen: Göttingen, Germany, **1997**.

[25] a) Gaussian 03, Revision C.02, M. J. Frisch, G. W. Trucks, H. B. Schlegel, G. E. Scuseria, M. A. Robb, J. R. Cheeseman, J. A., Jr., Montgomery, T. Vreven, K. N. Kudin, J. C. Burant, J. M. Millam, S. S. Iyengar, J. Tomasi, V. Barone, B. Mennucci, M. Cossi, G. Scalmani, N. Rega, G. A. Petersson, H. Nakatsuji, M. Hada, M. Ehara, K. Toyota, R. Fukuda, J. Hasegawa, M. Ishida, T. Nakajima, Y. Honda, O. Kitao, H. Nakai, M. Klene, X. Li, J. E. Knox, H. P. Hratchian, J. B. Cross, C. Adamo, J. Jaramillo, R. Gomperts, R. E. Stratmann, O. Yazyev, A. J. Austin, R. Cammi, C. Pomelli, J. W. Ochterski, P. Y. Ayala, K. Morokuma, G. A. Voth, P. Salvador, J. J. Dannenberg, V. G. Zakrzewski, S. Dapprich, A. D. Daniels, M. C. Strain, O. Farkas, D. K. Malick, A. D. Rabuck, K. Raghavachari, J. B. Foresman, J. V. Ortiz, Q. Cui, A. G. Baboul, S. Clifford, J. Cioslowski, B. B. Stefanov, G. Liu, A. Liashenko, P. Piskorz, I. Komaromi, R. L. Martin, D. J. Fox, T. Keith, M. A. Al-Laham, C. Y. Peng, A. Nanayakkara, M. Challacombe, P. M. W. Gill, B. Johnson, W. Chen, M. W. Wong, C. Gonzalez, J. A. Pople, Gaussian, Inc., Wallingford CT, **2004**; b) Gaussian 09, Revision A.1, M. J. Frisch, G. W. Trucks, H. B. Schlegel, G. E. Scuseria, M. A. Robb, J. R. Cheeseman, G. Scalmani, V. Barone, B. Mennucci, G. A. Petersson, H. Nakatsuji, M. Caricato, X. Li, H. P. Hratchian, A. F. Izmaylov, J. Bloino, G. Zheng, J. L. Sonnenberg, M. Hada, M. Ehara, K. Toyota, R. Fukuda, J. Hasegawa, M. Ishida, T. Nakajima, Y. Honda, O. Kitao, H. Nakai, T. Vreven, J. A., Jr., Montgomery, J. E. Peralta, F. Ogliaro, M. Bearpark, J. J. Heyd, E. Brothers, K. N. Kudin, V. N. Staroverov, R. Kobayashi, J. Normand, K. Raghavachari, A. Rendell, J. C. Burant, S. S. Iyengar, J. Tomasi, M. Cossi, N. Rega, N. J. Millam, M. Klene, J. E. Knox, J. B. Cross, V. Bakken, C. Adamo, J. Jaramillo, R. Gomperts, R. E. Stratmann, O. Yazyev, A. J. Austin, R. Cammi, C. Pomelli, J. W. Ochterski, R. L. Martin, K. Morokuma, V. G. Zakrzewski, G. A. Voth, P. Salvador, J. J. Dannenberg, S. Dapprich, A. D. Daniels, Ö. Farkas, J. B. Foresman, J. V. Ortiz, J. Cioslowski, D. J. Fox, Gaussian, Inc., Wallingford CT, **2009**.

[26] a) A. D. Becke, *J. Chem. Phys.* **1993**, *98*, 5648 – 5652; b) C. Lee, W. Yang, R. G. Parr, *Phys. Rev. B* **1988**, *37*, 785 – 789.

[27] a) A. E. Reed, L. A. Curtiss, F. Weinhold, *Chem. Rev.* **1988**, *88*, 899 – 926; b) E. D. Glendening, J. E. Reed, J. E. Carpenter, F. Weinhold, NBO Program 3.1; Madison, WI, **1988**.

Received: April 25, 2014
Published online on July 24, 2014